

Research on Stay Cable Tension Estimation Based on Vision-Based Monitoring System

Lusheng Wang*, Xin Gao

College of Construction Engineering, Jilin University, Changchun 130021, Jilin, China

*Correspondence Author, wangls22@mails.jlu.edu.cn

Abstract: *The cables in cable-stayed bridges are the primary load-bearing components, making the accurate monitoring of cable tension crucial for assessing the service reliability of the cables and the overall safety of the bridge. This study presents the development of a non-contact, vision-based monitoring system utilizing computer vision technology for monitoring cable tension in cable-stayed bridges. The monitoring system comprises an industrial camera equipped with an infrared filter and an infrared target lamp, employing a sub-pixel template matching algorithm to achieve high-precision cable tension measurement under long-distance and multi-frequency motion conditions. Model experiments were conducted to validate the accuracy and stability of the vision-based monitoring system. Results from long-distance model experiments indicate that the system can accurately measure frequencies across various distances, with a maximum frequency error of only 0.05%. Additionally, results from multi-frequency model experiments demonstrate that the system can accurately measure multiple vibration frequencies, with a maximum frequency error of just 0.4%.*

Keywords: Cable tension, Cable-stayed bridges, Computer vision, Structural health monitoring.

1. Introduction

The rapid advancement of technology and economic growth have driven a substantial rise in the construction of cable-stayed bridges, which are pivotal in modern transportation networks. Nevertheless, these bridges frequently encounter safety challenges arising from traffic loads and complex environmental conditions, underscoring the growing importance of structural health monitoring [1]. As the primary load-bearing component of cable-stayed bridges [2,3], cable reliability is the determining factor for the overall structural safety. Consequently, cable tension serves as a critical indicator for assessing both the cables' service condition and the bridge's overall safety [4,5]. Corrosion and fatigue can result in cable performance degradation [6,7], which subsequently compromises the structural stability of the bridge and poses safety risks [8]. Hence, regular inspections and continuous monitoring of cable tension are crucial to ensuring the safe operation of cable-stayed bridges [9,10].

Current methods for estimating cable tension can be broadly categorized into direct and indirect measurement methods [11,12]. Common direct measurement methods include the hydraulic jack method, the fiber Bragg grating (FBG) sensor, and the magnetic flux sensor. The hydraulic jack method is simple to operate but has relatively low accuracy and poses installation challenges, limiting its use primarily to bridge construction. The FBG sensor necessitates embedding the sensor within the cable during construction, rendering it unsuitable for bridges lacking pre-installed sensors. Although the magnetic flux provides high accuracy, it is highly susceptible to temperature variations and environmental factors. Since direct measurement approaches involve attaching sensors to the cable surface, they frequently present challenges in installation and wiring during practical applications.

The vibration frequency method, as an indirect measurement approach, has been widely applied in estimating cable tension in existing bridges due to its convenience and efficiency. This

method estimates cable tension by measuring the dynamic response of the cables and leveraging the relationship between the natural frequency and the geometric properties of the cables. Traditional contact sensors, such as accelerometers and displacement sensors, have been extensively used to measure the dynamic response of cables. However, in cable-stayed bridges with numerous cables, installing sensors and connecting them to the data acquisition system (DAQ) is both time-consuming and labor-intensive.

In response to the limitations of contact measurement methods, significant advancements have been made in non-contact measurement techniques in recent years, including laser Doppler technology, the Global Positioning System (GPS), and computer vision technology. Although laser Doppler technology provides high accuracy, it is expensive and involves complex wiring [13]. GPS is seldom employed for measuring bridge dynamic responses due to limitations in accuracy and sampling frequency [14]. In contrast, computer vision technology can measure structural dynamic responses using industrial or digital cameras. Computer vision technology has been widely used due to its significant advantages, such as low cost, ease of operation, easy installation, and multipoint measurements [15-17].

This study proposes a non-contact vision monitoring system based on computer vision algorithms, offering an effective solution for estimating cable tension in cable-stayed bridges.

2. Measurement Principles

2.1 Vision-based Monitoring System

The vision-based monitoring system employs a high-resolution industrial camera to capture videos of the cable's dynamic responses. The camera housing is waterproof, dustproof, and heat-insulated, ensuring reliable operation even in adverse weather conditions. Additionally, the camera is equipped with an infrared filter that exclusively allows infrared light to pass through. The system operates in conjunction with a powerful infrared target lamp, enabling

clear capture of the cable’s dynamic responses even in low-light and adverse weather conditions. Figure 1 details the key components of the vision-based monitoring system.



Figure 1: System components and specifications

2.2 Vibration Frequency Method

The vibration frequency method is widely used in engineering applications due to its simplicity and accuracy [18],[19]. It analyzes the dynamic response of the cable by extracting natural frequencies, subsequently estimating the cable tension based on the relationship between tension and natural frequencies. Since the in-plane and out-of-plane vibrations of the cable are not coupled, the analysis can be simplified to a planar problem. Additionally, by neglecting cable sag and considering bending stiffness as shown in Figure 2, the differential equation of motion for the cable can be expressed as equation (1).

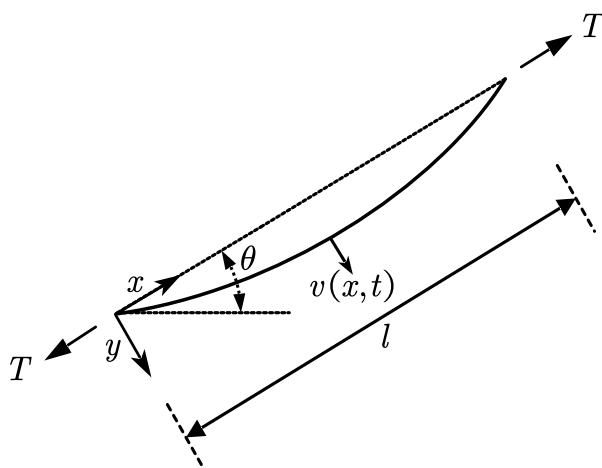


Figure 2: Model and parameters of the cable

$$EI \frac{\partial^4 v(x,t)}{\partial x^4} - T \frac{\partial^2 v(x,t)}{\partial x^2} + m \frac{\partial^2 v(x,t)}{\partial t^2} = 0 \tag{1}$$

In Eq. (2.1), where x represents the coordinate along the length of the cable, t represents time, $v(x, t)$ represents the displacement response in the vertical direction of the cable, m represents the mass per unit length of the cable, EI represents the bending stiffness of the cable, and T is the cable tension.

Under the assumption of hinged boundary conditions at both

ends of the cable, the solution to the differential equation in equation (1) can be expressed as equation (2).

$$T = 4ml^2 \left(\frac{f_n}{n}\right)^2 - \frac{\pi^2 EI}{l^2} n^2 \tag{2}$$

In equation (2), where l represents the effective length of the cable and f_n represents the n -th order frequency of the cable. If $(f_n/n)^2$ of equation (2) is expressed in the form of a first-order equation using the least squares method, the equation can be expressed as equation (3), and the cable tension can be calculated using equation (4). This method utilizes the natural frequencies of multiple vibration modes of the cable, which can partially correct the measurement errors, including those introduced by the unevenly distributed bending stiffness along the length direction.

$$\left(\frac{f_n}{n}\right)^2 = \frac{T}{4ml^2} + \frac{\pi^2 EI}{4ml^4} n^2 = b + a \cdot n^2 \tag{3}$$

$$T = 4ml^2 \cdot b \tag{4}$$

2.3 Template Matching Method

The template matching method is a classical computer vision technique used to identify the region in an image that best corresponds to a given template [20]. To reduce computation time, a predefined region of interest (ROI) in the reference frame is selected as the search area, and a matching criterion is applied to assess the similarity between the template image and subsets within the ROI. In this study, the zero-normalized cross-correlation (ZNCC) matching criterion is employed because it is robust against linear variations in illumination, leading to more accurate matching results. The $C(x, y)$ of the template image at the position (x, y) in the search region can be calculated by equation (5).

$$C(x, y) = \frac{\sum_{i=-M}^M \sum_{j=-N}^N \left[\frac{(f(x_i, y_j) - f_m)(g(x'_i, y'_j) - g_m)}{\Delta f \Delta g} \right]}{\sum_{i=-M}^M \sum_{j=-N}^N \left[\frac{(f(x_i, y_j) - f_m)(g(x'_i, y'_j) - g_m)}{\Delta f \Delta g} \right]} \tag{5}$$

$$f_m = \frac{\sum_{i=-M}^M \sum_{j=-N}^N f(x_i, y_j)}{(2M+1)(2N+1)} \tag{6}$$

$$g_m = \frac{\sum_{i=-M}^M \sum_{j=-N}^N g(x'_i, y'_j)}{(2M+1)(2N+1)} \tag{7}$$

$$\Delta f = \sqrt{\sum_{i=-M}^M \sum_{j=-N}^N (f(x_i, y_j) - f_m)^2} \tag{8}$$

$$\Delta g = \sqrt{\sum_{i=-M}^M \sum_{j=-N}^N (g(x'_i, y'_j) - g_m)^2} \tag{9}$$

In Eq. (2.6), $f(x_i, y_j)$ and $g(x'_i, y'_j)$ represent the pixel gray values at the specified positions in the region to be matched and the template image, respectively. f_m and g_m represent the average gray values of the region to be matched and the template image, respectively. Δf and Δg represent the standard deviation of the pixel gray values of the region to be matched and the template image, respectively. $(2M + 1)$ and $(2N + 1)$ represent the heights and widths of the region to be matched and the template image. The coordinate corresponding to the maximum value of the ZNCC $C(x, y)$ indicates the location of the most similar region to the template in the ROI, from which the displacement of the structure can be measured.

To determine the dynamic response of the structure, it is essential to establish the relationship between pixel displacement and structural displacement, referred to as the

scaling factor, as shown in equation (6). This can be calculated as the ratio of the physical dimensions to the corresponding pixel count.

$$x_s = SF \cdot x_p \quad (10)$$

$$SF = \frac{d_s}{d_p} \quad (11)$$

Where x_s represents the structure displacement, x_p represents the pixel displacement, and SF is the scaling factor, which can be calculated from the physical dimensions d_s of the measured structure and its pixels d_p in the image.

2.4 Subpixel Algorithm

When assessing the structural dynamic response, measurement accuracy is of paramount importance. Given that digital images are measured in pixels, pixel-level accuracy may be inadequate when the distance is significant or the camera resolution is low [21]. Consequently, sub-pixel interpolation is required to enhance resolution. Commonly used interpolation methods include nearest neighbor interpolation, bilinear interpolation, and bicubic interpolation. Among these, bilinear interpolation is frequently employed due to its high accuracy and computational efficiency [22]. Bilinear interpolation utilizes the grayscale values of four neighboring pixels surrounding the target pixel to perform linear interpolation in two directions, thereby enhancing resolution. The grayscale value of the sub-pixel point can be computed using equation (8).

$$f(x_i + u, y_j + v) = a + bu + cv + duv \quad (12)$$

The gray value of the desired sub-pixel point, $f(x_i + u, y_j + v)$, involves four parameters that can be determined by constructing a system of equations based on the gray values of the four surrounding pixel points, as shown in equation (9).

$$\begin{cases} a = f(x_i, y_j) \\ b = f(x_i + 1, y_j) - a \\ c = f(x_i, y_j + 1) - a \\ d = a + f(x_i + 1, y_j + 1) - b - c \end{cases} \quad (13)$$

2.5 Calculation Process of Cable Tension

First, the video captured by the industrial camera is converted into a time-ordered sequence of images. Based on the cable's vibration characteristics, a suitable ROI window is selected in the reference frame to expedite template matching. A template image is then chosen in the reference frame. Both the template image and ROI undergo preprocessing, where they are converted to grayscale and filtered to reduce noise. To enhance image resolution, bilinear sub-pixel interpolation is applied to the preprocessed template image and ROI. Template matching is performed by calculating the ZNCC to determine the optimal template match position within the ROI window for each frame, thereby calculating pixel displacement. This displacement is then converted to structural displacement using a scaling factor. Finally, the natural frequencies of each vibration mode of the cable are determined through PSD analysis of the cable displacement. These frequencies, excluding the first-order vibration mode, are applied to the vibration frequency method to calculate the cable tension.

3. Experimental Analysis

3.1 Experiment Setup

This study evaluates the performance of the proposed vision-based monitoring system using a programmable controlled linear slide module. As the vibration frequency method indicates, cable tension is closely related to its natural frequency, so this experiment aims to verify the frequency measurement accuracy under different experimental conditions, as shown in Figure 3. To measure the dynamic response of the linear slide module, a laser displacement sensor (LDS) and an infrared target lamp were installed on it. The industrial camera was used for video image acquisition, with the LDS synchronized at a sampling frequency of 50 Hz. Two experiments were conducted under different test scenarios. The first experiment verified the measurement accuracy of the vision-based monitoring system at different distances, thereby confirming the effectiveness of the sub-pixel algorithm. The second experiment assessed the system's accuracy in identifying multiple vibration frequencies.

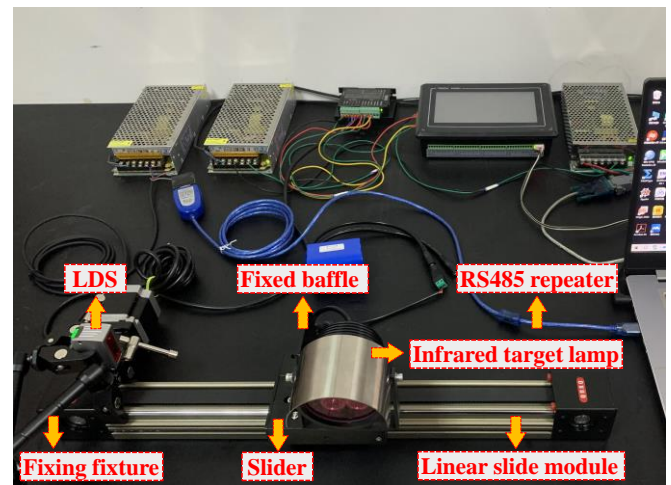


Figure 3: Experiment setup

3.2 Subpixel Experimental Verification

In practical engineering, the displacement measurement accuracy of the template matching method is often influenced by the measurement distance and camera resolution. Image resolution can be improved by using a high-resolution camera or reducing the measurement distance, but these approaches are often accompanied by high costs or are impractical in real-world operations. Therefore, more efficient sub-pixel interpolation techniques have been introduced to enhance image details. In this experiment, the bilinear interpolation sub-pixel algorithm was applied, and experiments were conducted at three different distances (15 m, 30 m, and 60 m). Since the motion of the linear slide is identical at different distances, the LDS selected only one of the measurement results as the reference value. The displacement measurement results are shown in Figure 4, and the frequency analysis results are shown in Figure 5.

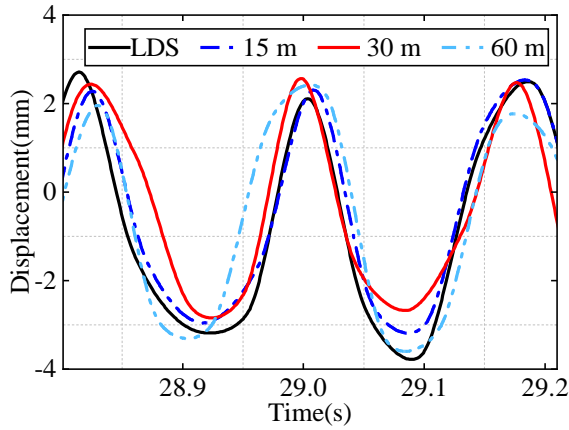


Figure 4: Displacements of different distances

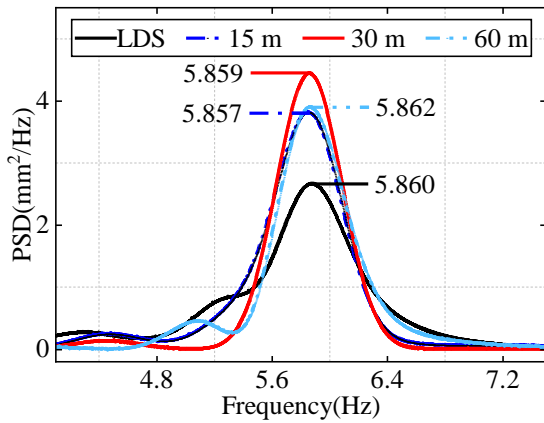


Figure 5: PSD of different distances

As shown in Figure 4 and Figure 5, the displacement measurement results and frequencies at different distances are generally consistent with those obtained by the LDS. To further validate the measurement accuracy of the vision-based monitoring system, an error analysis of the frequencies at different distances was conducted, and the results are presented in Table 1.

Table 1: Frequency error analysis

Conditions	Frequency (Hz)	Error (%)
LDS	5.860	/
15 m	5.857	0.05
30 m	5.859	0.02
60 m	5.862	0.03

As shown in Table 1, the frequency errors at different measurement distances are all below 0.05%, indicating that the bilinear interpolation sub-pixel algorithm used in this study maintains high measurement accuracy even at long distances.

3.3 Multi-frequency Validation

The vibration frequency method is an effective technique for measuring stay cable tension, where the accurate measurement of multiple vibration frequencies is particularly crucial. This method utilizes the least squares approach to fit a straight line to the obtained frequency data, thereby calculating the tension of the stay cables. To ensure high-precision measurement results, it is essential to capture the multiple vibration frequencies of the stay cables as accurately as possible in practical engineering applications, in order to minimize errors arising from inaccurate frequency measurements. Therefore, verifying the capability of the

vision-based monitoring system to accurately measure multiple vibration frequencies is particularly important. In this study, a motion scenario involving the superposition of four vibration frequencies was simulated using a linear slide module to test the accuracy of the vision-based monitoring system in measuring multiple vibration frequencies. The displacement measurement results are shown in Figure 6, and the frequency analysis results are shown in Figure 7.

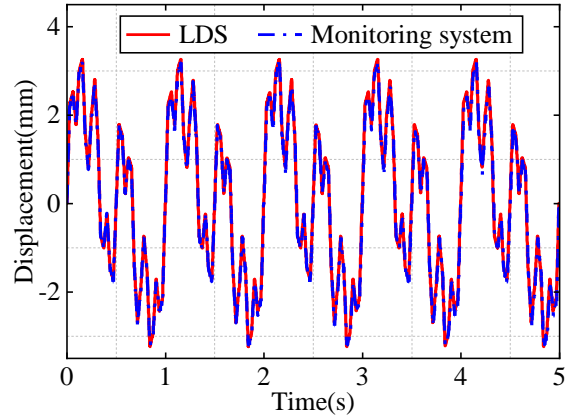


Figure 6: Displacements of multiple vibration frequencies

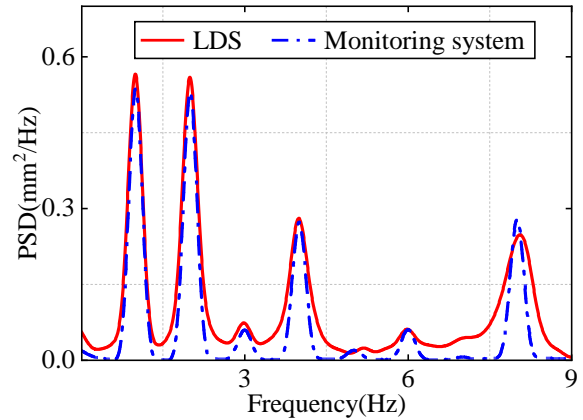


Figure 7: PSD of multiple vibration frequencies

As shown in Figure 6, the displacement results measured by the vision-based monitoring system for multi-frequency motion are nearly identical to those obtained by the LDS, demonstrating the accuracy of the system's displacement measurement. Figure 7 shows that the multiple vibration frequencies measured by the vision-based monitoring system are essentially the same as those measured by the LDS.

To further validate the accuracy of the vision-based monitoring system in measuring multiple vibration frequencies, an error analysis was conducted for each measured vibration frequency. The results of this analysis are presented in Table 2.

Table 2: Multiple frequencies error analysis

Frequency (Hz)	LDS	Monitoring system	Error (%)
1st	0.997	1.001	0.40
2nd	1.993	2.001	0.40
3rd	3.987	4.002	0.38
4th	7.974	8.005	0.39

As seen in Table 2, the vision-based monitoring system accurately measures the 4th-order vibration frequencies, with a maximum frequency error of only 0.4%. This clearly demonstrates the accuracy and stability of the system in

measuring multiple vibration frequencies.

4. Conclusion

To address the limitations of traditional contact measurement methods, this study proposes a non-contact, vision-based monitoring system utilizing computer vision algorithms to provide an effective solution for cable tension estimation in cable-stayed bridges. The reliability of the proposed vision-based monitoring system was validated through model experiments, leading to the following conclusions.

The sub-pixel experiment results indicate that the vision-based monitoring system is capable of achieving high-precision frequency measurements at various distances, maintaining accurate measurement precision at extended ranges, with a maximum frequency error of only 0.05%. The results demonstrate that the sub-pixel algorithm can effectively enhance measurement accuracy.

The multi-frequency experiment results indicate that the vision-based monitoring system can accurately identify the vibration frequencies of linear slide modules at various orders, with a maximum frequency error of only 0.4%. The results suggest that this system can be employed to measure the vibration frequencies of cables at different orders with precision.

Consequently, the vision-based cable tension monitoring system for cable-stayed bridges, as proposed in this study, attains sub-pixel measurement accuracy and offers reliable measurements over long distances and complex frequencies. The system effectively measures the displacement response and estimates the cable tension in a cost-efficient manner. This significantly enhances its practical utility, rendering it suitable for both routine inspections and long-term monitoring of cable tension.

References

- [1] J. T. Kim, T. C. Huynh and S. Y. Lee, Wireless structural health monitoring of stay cables under two consecutive typhoons, *Structural Monitoring and Maintenance*, 1(1), 47-67, 2014.
- [2] A. Camara, M. A. Astiz and A. J. Ye, Fundamental Mode Estimation for Modern Cable-Stayed Bridges Considering the Tower Flexibility, *Journal of Bridge Engineering*, 19(6), 04014015, 2014.
- [3] L. X. Zhang, G. Y. Qiu and Z. S. Chen, Structural health monitoring methods of cables in cable-stayed bridge: A review, *Measurement*, 168, 108343, 2021.
- [4] Y. Q. Bao, Z. Q. Shi, J. L. Beck, H. Li and T. Y. Hou, Identification of time-varying cable tension forces based on adaptive sparse time-frequency analysis of cable vibrations, *Structural Control & Health Monitoring*, 24(3), e1889, 2017.
- [5] Y. C. Yang, S. L. Li, S. Nagarajaiah, H. Li and P. Zhou, Real-Time Output-Only Identification of Time-Varying Cable Tension from Accelerations via Complexity Pursuit, *Journal of Structural Engineering*, 142(1), 04015083, 2016.
- [6] C. Jiang, C. Wu, C. S. Cai, X. Jiang and W. Xiong, Corrosion fatigue analysis of stay cables under combined loads of random traffic and wind, *Engineering Structures*, 206, 110153, 2020.
- [7] Y. B. Yang, K. Shi, Z. L. Wang, H. Xu, B. Zhang and Y. T. Wu, Using a Single-DOF Test Vehicle to Simultaneously Retrieve the First Few Frequencies and Damping Ratios of the Bridge, *International Journal of Structural Stability and Dynamics*, 21(8), 2150108, 2021.
- [8] A. Pipinato, C. Pellegrino, G. Fregno and C. Modena, Influence of Fatigue on Cable Arrangement in Cable-stayed Bridges, *International Journal of Steel Structures*, 12(1), 107-123, 2012.
- [9] S. W. Kim, B. G. Jeon, J. H. Cheung, S. D. Kim and J. B. Park, Stay cable tension estimation using a vision-based monitoring system under various weather conditions, *Journal of Civil Structural Health Monitoring*, 7(3), 343-357, 2017.
- [10] S. W. Kim, B. G. Jeon, N. S. Kim and J. C. Park, Vision-based monitoring system for evaluating cable tensile forces on a cable-stayed bridge, *Structural Health Monitoring-an International Journal*, 12(5-6), 440-456, 2013.
- [11] W. H. Wu, C. C. Chen, Y. C. Chen, G. Lai and C. M. Huang, Tension determination for suspenders of arch bridge based on multiple vibration measurements concentrated at one end, *Measurement*, 123, 254-269, 2018.
- [12] C. C. Chen, W. H. Wu, M. R. Leu and G. L. Lai, Tension determination of stay cable or external tendon with complicated constraints using multiple vibration measurements, *Measurement*, 86, 182-195, 2016.
- [13] H. H. Nassif, M. Gindy and J. Davis, Comparison of laser Doppler vibrometer with contact sensors for monitoring bridge deflection and vibration, *NDT & E International*, 38(3), 213-218, 2005.
- [14] M. R. Kaloop, Bridge safety monitoring based-GPS technique: case study Zhujiang Huangpu Bridge, *Smart Structures and Systems*, 9(6), 473-487, 2012.
- [15] X. W. Ye, C. Z. Dong and T. Liu, Force monitoring of steel cables using vision-based sensing technology: methodology and experimental verification, *Smart Structures and Systems*, 18(3), 585-599, 2016.
- [16] S. W. Kim, J. H. Cheung, J. B. Park and S. O. Na, Image-based back analysis for tension estimation of suspension bridge hanger cables, *Structural Control & Health Monitoring*, 27(4), 14, 2020.
- [17] B. F. Yan, D. R. Li, W. B. Chen, L. Deng and X. M. Jiang, Mode shape-aided cable force determination using digital image correlation, *Structural Health Monitoring-an International Journal*, 20(5), 2430-2445, 2021.
- [18] H. Li, W. L. Chen, F. Xu, F. C. Li and J. P. Ou, A numerical and experimental hybrid approach for the investigation of aerodynamic forces on stay cables suffering from rain-wind induced vibration, *Journal of Fluids and Structures*, 26(7-8), 1195-1215, 2010.
- [19] F. Benedettini and C. Gentile, Operational modal testing and FE model tuning of a cable-stayed bridge, *Engineering Structures*, 33(6), 2063-2073, 2011.
- [20] B. Pan, K. M. Qian, H. M. Xie and A. Asundi, Two-dimensional digital image correlation for in-plane displacement and strain measurement: a review,

Measurement Science and Technology, 20(6), 062001, 2009.

- [21] D. M. Feng and M. Q. Feng, Computer vision for SHM of civil infrastructure: From dynamic response measurement to damage detection – A review, *Engineering Structures*, 156, 105-117, 2018.
- [22] B. Pan, H. M. Xie, B. Q. Xu and F. L. Dai, Performance of sub-pixel registration algorithms in digital image correlation, *Measurement Science and Technology*, 17(6), 1615-1621, 2006.